

# The LHCb anomaly and $B$ physics in flavored $Z'$ models with flavored Higgs doublets

P. Ko<sup>1</sup>, Yuji Omura<sup>2</sup>, Yoshihiro Shigekami<sup>3</sup> and Chaehyun Yu<sup>4</sup>

<sup>1</sup>*School of Physics, KIAS, Seoul 02455, Korea*

<sup>2</sup>*Kobayashi-Maskawa Institute for the Origin of Particles and the Universe,  
Nagoya University, Nagoya 464-8602, Japan*

<sup>3</sup>*Department of Physics, Nagoya University, Nagoya 464-8602, Japan*

<sup>4</sup>*Department of Physics, Korea University, Seoul 02841, Korea*

## Abstract

We study an extended Standard Model with a gauged  $U(1)'$  flavor symmetry, motivated by not only the fermion mass hierarchy but also the excesses in  $B \rightarrow K^{(*)}ll$  reported by the LHCb collaborations. The  $U(1)'$  charges are assigned to quarks and leptons flavor-dependently and flavored Higgs doublets are also introduced to write down the Yukawa couplings at the renormalizable level. Then, the fermion mass hierarchy is realized by the vacuum alignment of the Higgs doublets. In this model, flavor changing currents involving the gauge boson of  $U(1)'$  and the scalars generated by the Higgs doublets are predicted and the observables in the  $B \rightarrow K^{(*)}ll$  process are possibly deviated from the Standard-Model predictions. We study the possibility that the new flavor changing interactions explain the excesses in the process, and we derive some predictions for the other flavor violating processes based on the analysis. We especially investigate the  $\Delta F = 2$  processes and the other  $B$  decays: e.g.,  $B \rightarrow X_s \gamma$  and  $B \rightarrow D^{(*)} \tau \nu$ , where the deviations are reported by the Belle and BaBar collaborations.

# 1 Introduction

The fermion mass hierarchy and the flavor mixing in the Standard Model (SM) are one of the mysteries in elementary particle physics, the origin of which one would like to understand. Top quark is much heavier than other fermions, and bottom quark and  $\tau$  lepton are also relatively heavy. On the other hand, electron, up and down quarks are much lighter than the other particles. Three active neutrinos are even much lighter than electron. Not only the mass spectra but also the flavor mixings show interesting patterns. Flavor mixing in the quark sector shows hierarchical structures, whereas those in the leptonic sector shows large mixings.

This hierarchical structure in the mass spectra may be a hint of new physics behind the SM. One well-known solution to explain the mass hierarchy is the Froggatt-Nielsen (FN) mechanism [1]. In this mechanism, flavor-dependent  $U(1)'$  symmetry is assigned to the SM fermions and the fermion mass hierarchy is realized by flavor-dependent suppressions generated by the flavor symmetry. The suppressions come from non-renormalizable higher-dimensional operators and the charge assignment of  $U(1)'$  is non-trivial. This mechanism is, however, known to explain well the hierarchy as well as the flavor mixings [1].

Inspired by the FN mechanism, we construct a model with  $U(1)'$  flavor gauge symmetry. In our model, we also introduce flavored Higgs doublet fields charged under the  $U(1)'$ , and then we write down the Yukawa couplings to generate the quarks and leptons mass matrices at the renormalizable level. Then, we claim that the vacuum alignment of the Higgs doublets is the origin of the fermion mass hierarchy. Note that we could derive the setup similar to the FN mechanism, integrating out the extra Higgs fields, so our setup proposes the origin of the higher-dimensional operators in the FN mechanism.

On the other hand, several excesses have been reported in the  $B$  decays by the LHCb collaboration. One is the lepton universality in the  $B \rightarrow Kll$  ( $l = e, \mu$ ) [2], and another is the angular distribution of  $B \rightarrow K^* \mu \mu$  [3, 4]. The global fitting analysis on the relevant Wilson coefficients has been done, including the  $B \rightarrow X_s \gamma$  process. Interestingly, the authors in Refs. [5–8] suggest the sizable operators,

$$C_9(\overline{s_L}\gamma_\mu b_L)(\overline{\mu}\gamma^\mu\mu) + C_{10}(\overline{s_L}\gamma_\mu b_L)(\overline{\mu}\gamma^\mu\gamma_5\mu) + h.c., \quad (1)$$

in order to explain the excesses. This may be a hint of new physics behind the hierarchical structure of the fermion masses.

In this work, we consider a charge assignment that left-handed quarks and  $\mu$  lepton are charged under  $U(1)'$ , and discuss the anomaly at the LHCb. Besides, we can expect that such a large new physics effect contributes to the other observables in flavor physics. We investigate the correlations and predictions in several flavor violating processes. As the authors of Refs. [9–11] pointed out, there are correlations between the  $Z'$  interaction from gauged  $U(1)'$  and scalar interaction from the Higgs fields, if we consider the explicit model with  $U(1)'$ . The large  $C_9$  and  $C_{10}$  might affect not only  $B \rightarrow K^{(*)}ll$  but also the other processes through the scalar interaction. Interesting physical observables are  $R(D^{(*)})$  that measures the flavor universality in the  $B \rightarrow D^{(*)}\tau\nu$  process. The experimental results at

the BaBar experiment are largely deviated from the SM prediction [12, 13]. The result reported by the Belle collaboration [14, 15] is closer to the SM prediction, but we still have a large tension between the experimental results and the prediction, so that this measurement motivates considering new particles that couple to bottom, charm quarks and  $\tau$  lepton or new physics in a model-independent way [16–58]. One good candidate is charged Higgs field as widely discussed [59–70] and it is realized in our model, as well. We study the compatibility between the excesses of  $B \rightarrow K^{(*)}ll$  and of  $B \rightarrow D^{(*)}\tau\nu$ , together with the consistency with  $B \rightarrow X_s\gamma$ .

This paper is organized as follows. In the next section, we introduce our model with the gauged  $U(1)'$  flavor symmetry, and present the  $Z'$  and scalar couplings with the SM fermions. Then, in Sec. 3 we study flavor physics:  $B \rightarrow K^{(*)}ll$ ,  $B \rightarrow D^{(*)}\tau\nu$ ,  $B \rightarrow X_s\gamma$  and so on. In Sec. 4, we introduce extra fields to make the flavor gauge symmetry anomaly-free, and propose dark matter candidates. Sec. 5 is devoted to the summary of our results.

## 2 Flavored $Z'$ models

Motivated by the fermion mass hierarchy and the excesses in the LHCb experiment, in this section we introduce our model with a gauged  $U(1)'$  flavor symmetry under which the SM fermions are charged. The  $U(1)'$  charges to the SM fermions are summarized in Table 1 and are chosen in such a manner that we can realize the fermion mass hierarchy and the sizable  $C_{9,10}$  that could resolve the LHCb anomalies. In principle there would be several possible charge assignments. The choice in Table 1 is motivated by the following points;

- The charges for the right-handed down-type quarks are universal, but  $C_9$  and  $C_{10}$  are generated by the flavor-dependent  $U(1)'$  charges of left-handed quarks. Flavor dependent gauge interactions in the left-handed quarks are strongly constrained by various flavor-changing neutral-current (FCNC) processes, which we will consider with great care in the following;
- The lepton flavor violating processes involving electron, such as  $\mu \rightarrow 3e$  and  $\mu \rightarrow e\gamma$ , are highly suppressed.

Different charge assignments would be also possible and similar phenomenology could be discussed in such a case as well.

Now we can write down the Yukawa couplings for the quarks and leptons,

$$\begin{aligned}
V_Y = & y_{1a}^u \overline{\hat{Q}_L^1} \widetilde{H}^a \hat{u}_R^a + y_{2a}^u \overline{\hat{Q}_L^2} \widetilde{H}^a \hat{u}_R^a + y_{33}^u \overline{\hat{Q}_L^3} \widetilde{H}^3 \hat{u}_R^3 + y_{32}^u \overline{\hat{Q}_L^3} \widetilde{H}^1 \hat{u}_R^2 \\
& + y_{ai}^d \overline{\hat{Q}_L^a} H^1 \hat{d}_R^i + y_{3i}^d \overline{\hat{Q}_L^3} H^2 \hat{d}_R^i \\
& + y_{11}^e \overline{\hat{L}^1} H^1 \hat{e}_R^1 + y_{AB}^e \overline{\hat{L}^A} H^2 \hat{e}_R^B + h.c.,
\end{aligned} \tag{2}$$

where  $a$  and  $b$  ( $A$  and  $B$ ) are the flavor indexes:  $a, b = 1, 2$  ( $A, B = 2, 3$ ). Depending on the definition of the  $U(1)'$  charges,  $q_i$  and  $q_e$ , additional Yukawa couplings would be

Fields	spin	SU(3) <sub>c</sub>	SU(2) <sub>L</sub>	U(1) <sub>Y</sub>	U(1)'
$\hat{Q}_L^a$	1/2	<b>3</b>	<b>2</b>	1/6	0
$\hat{Q}_L^3$	1/2	<b>3</b>	<b>2</b>	1/6	1
$\hat{u}_R^a$	1/2	<b>3</b>	<b>1</b>	2/3	$q_a$
$\hat{u}_R^3$	1/2	<b>3</b>	<b>1</b>	2/3	$1 + q_3$
$\hat{d}_R^i$	1/2	<b>3</b>	<b>1</b>	-1/3	$-q_1$
$\hat{L}^1$	1/2	<b>1</b>	<b>2</b>	-1/2	0
$\hat{L}^A$	1/2	<b>1</b>	<b>2</b>	-1/2	$q_e$
$\hat{e}_R^1$	1/2	<b>1</b>	<b>1</b>	-1	$-q_1$
$\hat{e}_R^A$	1/2	<b>1</b>	<b>1</b>	-1	$q_e - q_2$
$H^i$	0	<b>1</b>	<b>2</b>	1/2	$q_i$
$\Phi$	0	<b>1</b>	<b>1</b>	0	$q_\Phi$

Table 1: The charge assignment of the extra U(1)' symmetry.  $a$ ,  $A$  and  $i$  denote the flavor:  $a = 1, 2$ ,  $A = 2, 3$  and  $i = 1, 2, 3$ .  $q_2$  is defined as  $q_2 = q_1 + 1$ .

allowed to be written by the full gauge symmetry. We assume that the other Yukawa terms are forbidden by the gauge symmetry, adopting appropriate charge assignment of  $q_3$  and  $q_e$ . Note that  $\hat{Q}_L^i = (\hat{u}_L^i, \hat{d}_L^i)^T$ ,  $\hat{u}_R^i$ ,  $\hat{d}_R^i$  and  $\hat{e}_R^i$  are the left-handed, right-handed up-type, down-type quarks, and right-handed leptons in the flavor basis, respectively. The fields in the mass basis are described by  $u^i$ ,  $d^i$  and  $e^i$  and correspond to the quarks and leptons as  $(u^1, u^2, u^3) = (u, c, t)$ ,  $(d^1, d^2, d^3) = (d, s, b)$  and  $(e^1, e^2, e^3) = (e, \mu, \tau)$ , respectively.

The mass eigenstates can be defined after the electroweak (EW) and U(1)' symmetry breaking. As shown in Table 1, “three” flavored Higgs doublets,  $H^i$ , and one U(1)'-charged scalar ( $\Phi$ ) are introduced and they break the gauge symmetries developing non-vanishing vacuum expectation values (VEVs). Only Higgs doublets can spontaneously break both EW and U(1)' symmetry, but  $\Phi$  is also required to avoid the strong bound from the constraints on the electroweak precision observables (EWPOs) and the heavy resonance search. According to the charge assignment in Table 1, the renormalizable scalar potential invariant under the assumed gauge symmetries can be written down as

$$\begin{aligned}
V_H = & m_{H_i}^2 |H_i|^2 + m_\Phi^2 |\Phi|^2 + \lambda_H^{ij} |H_i|^2 |H_j|^2 + \lambda_{H\Phi}^i |H_i|^2 |\Phi|^2 + \lambda_\Phi |\Phi|^4 \\
& - A_1 H_1^\dagger H_2 (\Phi)^{\frac{q_1 - q_2}{q_\Phi}} - A_2 H_2^\dagger H_3 (\Phi)^{\frac{q_2 - q_3}{q_\Phi}} - A_3 H_1^\dagger H_3 (\Phi)^{\frac{q_1 - q_3}{q_\Phi}} + h.c., \quad (3)
\end{aligned}$$

where  $q_\Phi$  is the charge of  $\Phi$ . In order to realize the fermion mass hierarchy through the Higgs VEVs, we require that the size of each Higgs VEV satisfies the following relation:

$$\langle H_1 \rangle \ll \langle H_2 \rangle \ll \langle H_3 \rangle. \quad (4)$$

Let us define  $q_\Phi$  as  $-1$  and assume that  $m_{H_1}$  is much heavier than the EW scale. In this setup,  $H_1$  could be integrated out and then the effective lagrangian would be the Two Higgs doublet model (2HDM) with  $H_{2,3}$  and  $\Phi$ . The Yukawa couplings could be then described by replacing  $H_1$  with the higher dimensional term involving  $\Phi$  as follows:

$$H_1 \rightarrow \frac{A_1}{m_{H_1}^2} \Phi H_2. \quad (5)$$

Note that  $H_2$  and  $H_3$  as well as  $\Phi$  will develop non-vanishing VEVs. Then, we define the vacuum alignment of the neutral components as

$$\langle H_2 \rangle = \frac{v}{\sqrt{2}} \cos \beta, \quad \langle H_3 \rangle = \frac{v}{\sqrt{2}} \sin \beta, \quad \langle \Phi \rangle = \frac{v_\Phi}{\sqrt{2}}, \quad (6)$$

and discuss the phenomenology, depending on the vacuum alignment. Note that the explanation of the fermion mass hierarchy through the VEVs requires large  $\tan \beta$ .

There are still many possible charge assignments for  $q_i$ ,  $q_e$  and  $q_\Phi$ . In order to evade the bound from the Drell-Yan process and write down  $A_{1,2}$  terms at the renormalizable level, we define the charges as  $(q_1, q_2, q_3, q_\Phi) = (0, 1, 3, -1)$ . The condition for  $q_3$  forbids  $A_3$  term at the renormalizable level.  $q_e$  is treated as a free parameter and we chose  $q_e$  that can enhance  $B \rightarrow K^{(*)} ll$ .

## 2.1 The fermion mass matrices

After the EW and  $U(1)'$  symmetry breaking, the mass matrices for the quarks and charged leptons are generated as follows:

$$\frac{v}{\sqrt{2}} Y_{ij}^u \hat{u}_L^i \hat{u}_R^j + \frac{v}{\sqrt{2}} Y_{ij}^d \hat{d}_L^i \hat{d}_R^j + \frac{v}{\sqrt{2}} Y_{ij}^e \hat{e}_L^i \hat{e}_R^j, \quad (7)$$

where each matrix,  $Y_{ij}^{u,d,e}$ , is defined as

$$(Y_{ij}^u) = \begin{pmatrix} y_{11}^u \epsilon & y_{12}^u & 0 \\ y_{21}^u \epsilon & y_{22}^u & 0 \\ 0 & y_{32}^u \epsilon & y_{33}^u \end{pmatrix} \begin{pmatrix} \cos \beta & & \\ & \cos \beta & \\ & & \sin \beta \end{pmatrix}, \quad (8)$$

$$(Y_{ij}^d) = \cos \beta \begin{pmatrix} \epsilon & & \\ & \epsilon & \\ & & 1 \end{pmatrix} \begin{pmatrix} y_{11}^d & y_{12}^d & y_{13}^d \\ y_{21}^d & y_{22}^d & y_{23}^d \\ y_{31}^d & y_{32}^d & y_{33}^d \end{pmatrix}, \quad (9)$$

and

$$(Y_{ij}^e) = \cos \beta \begin{pmatrix} \epsilon & & \\ & 1 & \\ & & 1 \end{pmatrix} \begin{pmatrix} y_{11}^e & 0 & 0 \\ 0 & y_{22}^e & y_{23}^e \\ 0 & y_{32}^e & y_{33}^e \end{pmatrix}. \quad (10)$$

$\epsilon$  comes from the contributions of  $\langle H_1 \rangle$ , and is given by

$$\epsilon = \frac{A_1}{m_{H_1}^2} \langle \Phi \rangle. \quad (11)$$

Using the diagonalizing unitary matrices, the mass matrices are given by

$$\frac{v}{\sqrt{2}} Y^I = (U_L^I)^\dagger \text{diag}(m_1^I, m_2^I, m_3^I) U_R^I \quad (I = u, d, e). \quad (12)$$

Assuming the hierarchical VEV alignment in Eq. (4), the fermion mass hierarchy can be obtained. For instance, the ratios of the up-type quark masses are approximately evaluated from  $Y^u$ :

$$m_c/m_t = \mathcal{O}(y_{22}^u/y_{33}^u \tan \beta), \quad m_u/m_c = \mathcal{O}(\epsilon y_{11}^u/y_{22}^u). \quad (13)$$

As we will discuss in flavor physics,  $\tan \beta$  is strongly constrained by  $B$  physics, so that we expect that the small  $y_{22}^u$  compensates the mass hierarchy. In addition, the mass hierarchy between  $m_u$  and  $m_c$  is larger than the other elements in the first and second generations. Then, we assume that  $y_{11}^u/y_{22}^u$  is  $\mathcal{O}(0.1)$  in our study.  $\epsilon$  explain the mass hierarchy in the down-type quark and lepton sector:

$$m_s/m_b = \mathcal{O}(\epsilon), \quad m_e/m_\mu = \mathcal{O}(\epsilon). \quad (14)$$

We still need some tuning of the parameters for the hierarchies between strange and down quarks ( $\tau$  and  $\mu$  leptons) and especially (1, 2)-elements of the CKM matrix, but this charge assignment and setup can fit the realistic mass matrices to a good approximation, and can evade the strong constraints from flavor physics suppressing the tree-level FCNCs, as we see below.

We can also estimate  $U_L^I$  and  $U_R^I$  that are the unitary matrices to diagonalize the mass matrices. They are relevant to the FCNCs of  $Z'$  and scalars. Based on the above discussion, we can estimate the size of each element of the unitary matrices according to the hierarchical structures. The elements, which are important in our study on flavor physics, are given by

$$|(U_L^d)_{33}| \simeq 1, \quad |(U_L^d)_{23}| = \mathcal{O}(\epsilon), \quad |(U_L^d)_{13}| = \mathcal{O}(\epsilon), \quad (15)$$

and

$$|(U_R^u)_{33}| \simeq 1, \quad |(U_R^u)_{23}| = \mathcal{O}(\epsilon), \quad |(U_R^u)_{23}| \gg |(U_R^u)_{13}|. \quad (16)$$

## 2.2 $Z'$ couplings

Let us discuss the gauged  $U(1)'$  interaction in this subsection. Based on Table 1, the  $Z'$  gauge couplings in the flavor basis are given by

$$\begin{aligned} \mathcal{L}_{Z'} = & g' \hat{Z}'_\mu \left( \hat{Q}_L^3 \gamma^\mu \hat{Q}_L^3 + q_1 \bar{\hat{u}}_R^1 \gamma^\mu \hat{u}_R^1 + (1 + q_1) \bar{\hat{u}}_R^2 \gamma^\mu \hat{u}_R^2 + q_3 \bar{\hat{u}}_R^3 \gamma^\mu \hat{u}_R^3 \right) \\ & + g' \hat{Z}'_\mu \left( q_e \bar{\hat{L}}^A \gamma^\mu \hat{L}^A - q_1 \bar{\hat{d}}_R^1 \gamma^\mu \hat{d}_R^1 - q_1 \bar{\hat{e}}_R^1 \gamma^\mu \hat{e}_R^1 + (q_e - q_2) \bar{\hat{e}}_R^A \gamma^\mu \hat{e}_R^A \right). \end{aligned} \quad (17)$$

After the EW and  $U(1)'$  symmetry breaking, we obtain the mass eigenstates and the  $Z'$  couplings to the SM fermions in the mass eigenstates are described as

$$\begin{aligned}\mathcal{L}_{Z'} = & g' \hat{Z}'_\mu \left\{ (g_L^u)_{ij} \overline{u_L^i} \gamma^\mu u_L^j + (g_L^d)_{ij} \overline{d_L^i} \gamma^\mu d_L^j + (g_R^u)_{ij} \overline{u_R^i} \gamma^\mu u_R^j - q_1 \overline{d_R^i} \gamma^\mu d_R^i \right\} \\ & + g' \hat{Z}'_\mu \left\{ q_e (\overline{\mu_L} \gamma^\mu \mu_L + \overline{\tau_L} \gamma^\mu \tau_L) + (g_L^\nu)_{ij} \overline{\nu_L^i} \gamma^\mu \nu_L^j - q_1 \overline{e_R^1} \gamma^\mu e_R^1 + (q_e - q_2) \overline{e_R^A} \gamma^\mu e_R^A \right\}.\end{aligned}\quad (18)$$

Each coupling in Eq. (17) is defined as

$$(g_L^d)_{ij} = (U_L^d)_{i3} (U_L^d)_{j3}^*, \quad (19)$$

$$(g_L^u)_{ij} = (U_L^u)_{i3} (U_L^u)_{j3}^* = (V_{CKM})_{ik} (g_L^d)_{kk'} (V_{CKM})_{jk'}^*, \quad (20)$$

$$(g_R^u)_{ij} = (U_R^u)_{ik} q_k (U_R^u)_{jk}^*, \quad (21)$$

$$(g_L^\nu)_{ij} = q_e^k \{ (U_L^\nu)_{ik} (U_L^\nu)_{jk}^* \} = q_e \left\{ \delta_{ij} - (V_{PMNS}^\dagger)_{i3} (V_{PMNS}^\dagger)_{j3}^* \right\}. \quad (22)$$

Note that the GIM mechanism does not work here for  $Z'$  gauge interactions, since  $U(1)'$  gauge symmetry is flavor-dependent in our model. There will be generic FCNC interactions involving  $Z'$  in the mass eigenstates of the SM fermions. Based on the estimation of the diagonalizing matrices, we find that the FCNCs are roughly evaluated as

$$\begin{aligned}(g_L^d)_{sb} = \mathcal{O}(\epsilon), \quad (g_L^d)_{db} = \mathcal{O}(\epsilon), \quad (g_L^d)_{sd} = \mathcal{O}(\epsilon^2), \\ (g_L^u)_{ij} \simeq (g_L^d)_{ij}, \quad (g_R^u)_{ct} = q_3 \times \mathcal{O}(\epsilon), \quad |(g_R^u)_{ct}| \gg |(g_R^u)_{ut}|, \quad |(g_R^u)_{uc}|.\end{aligned}\quad (23)$$

In addition,  $\hat{Z}'_\mu$  mixes with  $\hat{Z}_\mu$  originated from  $SU(2)_L \times U(1)_Y$ , through the mass mixing generated by non-vanishing VEVs of  $H_i$ . The mixing is suppressed by  $v_\Phi$  and should be tiny to evade the strong bound concerned with the  $\rho$ -parameter. Such a tiny mixing can be achieved by the assumption that  $v_\Phi$  dominates the  $Z'$  mass ( $M_{Z'}$ ).

Assuming the  $U(1)'$  coupling  $g'$  is comparable with the  $Z$  boson coupling, we find that the constraint from the  $\rho$ -parameter leads to the bound on  $\Lambda_{Z'} \equiv M_{Z'}/g'$ :

$$\Lambda_{Z'} \gtrsim 23.3 \text{ TeV} \times \left( \frac{q_3}{3} \right) \times \left( \frac{10^{-3}}{\Delta\rho_{\max}} \right)^{\frac{1}{2}}, \quad (24)$$

when  $\tan \beta$  is large.  $\Delta\rho_{\max}$  is the upper bound on the  $\rho$ -parameter and roughly estimated as  $\mathcal{O}(10^{-3})$  [71].

### 2.3 Yukawa couplings

After the EW and  $U(1)'$  symmetry breaking, a number of scalar bosons appear as physical modes from the Higgs fields. In the limit that the scalars of  $\Phi$  are much heavier than the others, we find 2 CP-even scalars,  $h$  and  $H$ , CP-odd scalar,  $A$ , and charged Higgs fields,  $H^\pm$ . There are also extra CP-even and CP-odd scalars from the fields charged under  $U(1)'$ , such as  $\Phi$ ,  $\Phi_l$  and  $\Phi_r$  introduced in Tables 1 and 4. Assuming that the

mixing between the scalar fields from the Higgs fields and the SM-singlet fields is not significantly large, the Yukawa couplings of these scalar bosons with the SM fermions in the mass basis are given by

$$-\mathcal{L}_Y = (Y_S^u)_{ij} S \overline{u}_L^i u_R^j + (Y_S^d)_{ij} h \overline{d}_L^i d_R^j + (Y_S^e)_{ij} H \overline{e}_L^i e_R^j \\ + (Y_\pm^u)_{ij} H^- \overline{d}_L^i u_R^j + (Y_\pm^d)_{ij} H^+ \overline{u}_L^i d_R^j + (Y_\pm^e)_{ij} H^+ \overline{\nu}_L^i e_R^j + h.c., \quad (25)$$

where  $S$  denotes three neutral scalar fields:  $S = h, H, A$ , and  $H^\pm$  denote the charged Higgs fields. In our model, each Yukawa coupling is given as follows:

$$(Y_h^u)_{ij} = \frac{m_u^i \sin(\alpha - \beta)}{v} G_{ij} + \frac{m_u^i \cos(\alpha - \beta)}{v} \delta_{ij}, \quad (26)$$

$$(Y_H^u)_{ij} = \frac{m_u^i \cos(\alpha - \beta)}{v} G_{ij} - \frac{m_u^i \sin(\alpha - \beta)}{v} \delta_{ij}, \quad (27)$$

$$(Y_A^u)_{ij} = -i \frac{m_u^i}{v} G_{ij}, \quad (28)$$

$$(Y_\pm^u)_{ij} = -\frac{m_u^k \sqrt{2}}{v} V_{ki}^* G_{kj}, \quad (29)$$

and

$$(Y_h^d)_{ij} = -\delta_{ij} \frac{m_d^i \cos \alpha}{v \cos \beta}, \quad (30)$$

$$(Y_H^d)_{ij} = \delta_{ij} \frac{m_d^i \sin \alpha}{v \cos \beta}, \quad (31)$$

$$(Y_A^d)_{ij} = -i \delta_{ij} \frac{m_d^i}{v} \tan \beta, \quad (32)$$

$$(Y_\pm^d)_{ij} = -V_{ij} \frac{m_d^j \sqrt{2}}{v} \tan \beta. \quad (33)$$

$(Y_S^e)_{ij}$  and  $(Y_\pm^e)_{ij}$  are given by replacing  $m_d^i$  and  $V_{ij}$  with  $m_e^i$  and  $(V_{PMNS})_{ji}^*$  in  $(Y_S^d)_{ij}$  and  $(Y_\pm^d)_{ij}$ , respectively.  $G_{ij}$  is originated from the flavor gauge symmetry, and described as

$$G_{ij} = \left( U_R^u \begin{pmatrix} -\tan \beta & & \\ & -\tan \beta & \\ & & \frac{1}{\tan \beta} \end{pmatrix} U_R^{u\dagger} \right)_{ij} \\ = -\tan \beta \delta_{ij} + \left( \tan \beta + \frac{1}{\tan \beta} \right) (G_R^u)_{ij}, \quad (34)$$

where  $(G_R^u)_{ij}$  is defined by  $(G_R^u)_{ij} \equiv (U_R^u)_{i3} (U_R^u)_{j3}^*$ . Because  $G_{ij} \propto \delta_{ij}$  is no longer true in the presence of flavor-dependent  $U(1)'$  gauge interactions, there appear non-minimal flavor-violating (non-MFV) scalar interactions, which was first noticed in Refs. [9, 10]. These new interactions are absent in the usual 2HDMs with softly broken  $Z_2$  symmetries,



$\alpha_s(M_Z)$	0.1193(16) [71]	$\lambda$	0.22537(61) [71]
$G_F$	$1.1663787(6) \times 10^{-5} \text{ GeV}^{-2}$ [71]	$A$	$0.814^{+0.023}_{-0.024}$ [71]
$m_b$	$4.18 \pm 0.03 \text{ GeV}$ [71]	$\bar{\rho}$	0.117(21) [71]
$m_t$	$160^{+5}_{-4} \text{ GeV}$ [71]	$\bar{\eta}$	0.353(13) [71]
$m_c$	$1.275 \pm 0.025 \text{ GeV}$ [71]		

Table 2: The input parameters relevant to our analyses. The CKM matrix,  $V$ , is written in terms of  $\lambda$ ,  $A$ ,  $\bar{\rho}$  and  $\bar{\eta}$  [71].

and could play an important role in understanding the flavor-nonuniversal phenomena through flavor-dependent gauge and scalar interactions [9–11]. Based on the estimation of  $(U_R^u)_{i3}$  in Eq. (16), we obtain

$$(G_R^u)_{tt} \simeq 1, |(G_R^u)_{tc}| \simeq \mathcal{O}(\epsilon), |(G_R^u)_{tc}| \gg |(G_R^u)_{ut}|, |(G_R^u)_{uc}|. \quad (35)$$

Then, we find that  $(Y_S^u)_{tc}$  and  $(Y_{\pm}^u)_{bc}$  are relatively larger and the other elements except for  $(Y_S^u)_{tt}$  are highly suppressed. This is very interesting because the Belle and BaBar collaborations reported some excess in  $B \rightarrow D^{(*)}\tau\nu$  [13–15]. In Sec. 3, we will study this excess together with relevant observables.

Note that the constraint on the EWPOs as well as the Higgs signals has been investigated at the one-loop level in 2HDM with  $U(1)'$  gauge symmetry, where the Higgs fields are charged under  $U(1)'$  [72]. The degenerate spectrum of the scalar fields and  $\cos(\alpha - \beta) \sim 1$  are also required, in addition to the constraint in Eq. (24). In our analysis of flavor physics, we assume that the scalar fields except for  $h$  are almost degenerate and  $\cos(\alpha - \beta)$  is close to unity.

### 3 Flavor physics involving $b$ quark

Based on the setup and interactions derived in the previous section, we shall study relevant flavor physics:  $B \rightarrow K^{(*)}ll$ , the  $\Delta F = 2$  processes,  $B \rightarrow X_s\gamma$ , and  $B \rightarrow D^{(*)}\tau\nu$ . The input parameters are summarized in Table 2.

#### 3.1 $b \rightarrow sll$ and $\Delta F=2$ processes

First, we consider the  $b \rightarrow sll$  ( $l = e, \mu$ ) decays. In this model, tree-level  $Z'$  exchanging diagrams contribute to the flavor violating processes,  $b \rightarrow sll$ . In the  $\Delta B = 1$  effective Hamiltonian, the relevant tree-level contributions are given by

$$\mathcal{H}_{\text{eff}} = -g_{\text{SM}} [C_9^l(\bar{s}_L\gamma_\mu b_L)(\bar{l}\gamma^\mu l) + C_{10}^l(\bar{s}_L\gamma_\mu b_L)(\bar{l}\gamma^\mu\gamma_5 l) + h.c.], \quad (36)$$

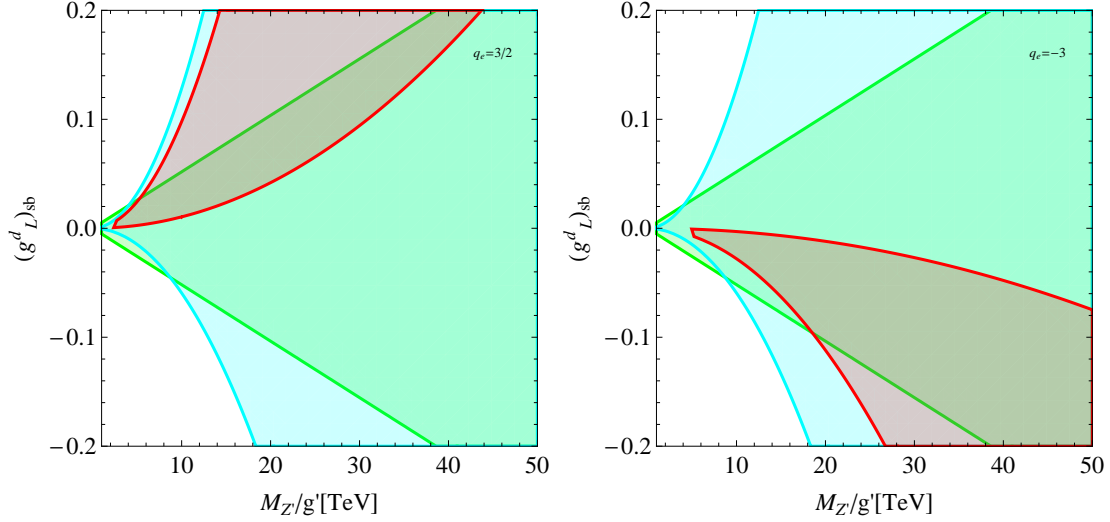


Figure 1:  $M_{Z'}/g'$  vs.  $(g_L^d)_{sb}$  for  $q_e = \frac{3}{2}$  (left panel) and  $q_e = -3$  (right panel), respectively. The red and blue regions are allowed by the global fits of  $C_9^\mu$  and  $C_{10}^\mu$  within  $1\sigma$ , respectively. The green region is allowed by the  $B_s$ - $\bar{B}_s$  mixing within  $1\sigma$ .

where  $C_9^l$  and  $C_{10}^l$  are given by

$$C_9^e = C_{10}^e = \frac{g'^2}{2g_{\text{SM}}M_{Z'}^2}(g_L^d)_{sb}q_1, \quad (37a)$$

$$C_9^\mu = C_9^\tau = -\frac{g'^2}{2g_{\text{SM}}M_{Z'}^2}(g_L^d)_{sb}(2q_e - q_2), \quad (37b)$$

$$C_{10}^\mu = C_{10}^\tau = \frac{g'^2}{2g_{\text{SM}}M_{Z'}^2}(g_L^d)_{sb}q_2, \quad (37c)$$

and the SM contributions are omitted.  $g_{\text{SM}}$  is the factor from the SM contribution:

$$g_{\text{SM}} = \frac{4G_F}{\sqrt{2}}V_{tb}V_{ts}^*\frac{e^2}{16\pi^2}. \quad (38)$$

It is real to a good approximation. We note that the Wilson coefficients in Eqs. (37) are flavor-dependent. Since we set  $q_1 = 0$  and  $q_2 = 1$ , the process  $b \rightarrow see$  is not affected by the  $Z'$  exchange at the tree level. The process  $b \rightarrow s\tau\tau$  will be also affected in our model, but we do not consider the processes because of the lack of experimental data.

In the LHCb experiment, a few discrepancies between the experimental results and the SM predictions have been reported in the  $b \rightarrow sll$  decays. One of them is the flavor universality in the  $B \rightarrow Kll$  decays [2], where the discrepancy in the  $l = \mu$  and  $l = e$  channels is about  $2.6\sigma$ . Another interesting anomaly which was reported by the LHCb Collaboration is the angular observable  $P'_5$  in the  $B \rightarrow K^*\mu^+\mu^-$  with a  $3.4\sigma$  deviation [3, 4].

Motivated by these discrepancies, a lot of works have been performed so far with new physics, in particular, flavor-dependent  $Z'$  boson [36, 42, 73–77], which is realized in this work. In order to restrict the Wilson coefficients (37), we adopt the results of the model-independent analysis in the framework of global fits in the space of Wilson coefficients to available data on the  $b \rightarrow sll$  decays which include  $B \rightarrow Kll$ ,  $B \rightarrow K^*ll$ ,  $B_s \rightarrow \phi ll$ ,  $B_s \rightarrow ll$  and/or  $b \rightarrow s\gamma$  processes [5–8]. We take the result in Ref. [8] for  $C_9^e = C_{10}^e = 0$ . The ratios of the Wilson coefficients with new physics to those in the SM are allowed in the range of

$$-0.29 (-0.34) \leq C_9^\mu/C_9^{\text{SM}} \leq -0.013 (0.053), \quad (39a)$$

$$-0.19 (-0.29) \leq C_{10}^\mu/C_{10}^{\text{SM}} \leq 0.088 (0.15) \quad (39b)$$

at the  $1\sigma$  ( $2\sigma$ ) level, respectively [8]. In Fig. 1, we depict the allowed region of  $M_{Z'}/g'$  and  $(g_L^d)_{sb}$  for  $q_e = \frac{3}{2}$  (left panel) and  $q_e = -3$  (right panel), respectively. The red and blue regions are allowed by the global fits in Eqs. (39) for  $C_9^\mu$  and  $C_{10}^\mu$  at the  $1\sigma$  level, respectively. As shown in Fig. 1,  $C_9^\mu$  is much more constrained than  $C_{10}^\mu$ . Note that there is a lower bound on  $M_{Z'}/g'$  from the  $\rho$  parameter, as shown in Eq. (24). For  $M_{Z'}/g' \gtrsim 20$  TeV, we find that the allowed regions require a sizable mixing  $|(g_L^d)_{sb}| \gtrsim 0.01$  in both cases.

Next, we consider the  $\Delta F = 2$  process. The  $Z'$ -mediated FCNCs are strongly constrained by the  $B_s$ - $\bar{B}_s$  mixing. The relevant effective Hamiltonian for  $\Delta F = 2$  with the  $Z'$  exchange is

$$\mathcal{H}_{\text{eff}}^{\Delta F=2} = C_1^{ij} (\bar{d}_L^i \gamma_\mu d_L^j) (\bar{d}_L^i \gamma_\mu d_L^j), \quad (40)$$

where  $C_1^{ij}$  is

$$C_1^{ij} = \frac{g'^2}{2M_{Z'}^2} (g_L^d)_{ij} (g_L^d)_{ij}. \quad (41)$$

The SM contribution  $C_1^{ij, \text{SM}}$  is omitted again. We note that the right-handed  $Z'$  exchange can also generate the  $\Delta F = 2$  process [78–80], but in this model that those contribution is suppressed by small mixings in  $(g_R^d)_{ij}$ , as shown in Eq. (23). The heavy Higgs exchange also generates extra contributions, but it could vanish in the SM limit and the assumption of the small scalar mass difference:  $\cos(\beta - \alpha) = 1$  and  $m_H = m_A$ . This condition is required by the EWPOs, as mentioned in the end of Sec. 2.

In the SM, the mass difference of the  $B_{1,2} \equiv (B_s \pm \bar{B}_s)/\sqrt{2}$  mesons is obtained as

$$\Delta m_s = \frac{G_F^2}{6\pi^2} m_{B_s} f_{B_s}^2 \hat{B}_{B_s} \eta m_W^2 |V_{tb}^* V_{ts}|^2 S_0(x_t), \quad (42)$$

where we ignore the small imaginary part in the CKM matrix elements, and the function  $S(x_t)$  with  $x_t = m_t^2/m_W^2$  can be found in Ref. [81]. The QCD correction factor  $\eta = 0.551$  and  $f_{B_s} \hat{B}_{B_s}^{1/2} = 0.266 \pm 0.018$  [82], where  $f_{B_s}$  is the decay constant of the  $B_s$  meson and  $\hat{B}_{B_s}$  is the bag parameter. The averaged value for the measured  $\Delta m_s$  is  $\Delta m_s = 17.757 \pm 0.021$  ps $^{-1}$  [83]. We note that the uncertainties in  $f_{B_s} \hat{B}_{B_s}^{1/2}$  dominate over those in the other parameters as well as in the  $\Delta m_s$ . In Fig. 1, the green region corresponds to the allowed

one by  $\Delta m_s$  at the  $1\sigma$  level. One can find the region which is in agreement with the global fits in the  $b \rightarrow sll$  processes and  $\Delta m_s$  simultaneously for both  $q_e = 3/2$  and  $q_e = -3$ . However we find that there is no allowed region for small  $q_e$ , for example,  $q_e = 1/2$  at the  $1\sigma$  level. For  $M_{Z'}/g' \sim 20$  TeV, the upper bound on  $(g_L^d)_{sb}$  is estimated as

$$0.04(0.01) \lesssim |(g_L^d)_{sb}| \lesssim 0.1(0.1) \quad (43)$$

for both  $q_e = 3/2$  ( $-3$ ), respectively.

Since the scalar potential in our model is approximated to be the 2HDM at the EW scale, the charged Higgs boson also contribute to the  $B_s$ - $\bar{B}_s$  mixing through box diagrams [61, 84]. We find that those contribution could be large for small  $\tan\beta$  or large  $(G_R^u)_{tc}$ , but it can be negligible for  $\tan\beta \gtrsim 5$  and  $(G_R^u)_{tc} \lesssim 0.1$ .

In addition to the  $B_s$ - $\bar{B}_s$  mixing, other  $\Delta F = 2$  processes also require the suppressed off-diagonal elements of  $(g_L^d)_{ij}$ . Assuming that  $(g_L^d)_{ij}$  have the same phase as  $(V_{ti}^* V_{tj})^2$ , we obtain the strong bounds on the (d, b) and (s, d) elements of  $(g_L^d)_{ij}$ :

$$|(g_L^d)_{db}| \lesssim 8.54 \times 10^{-4} \left( \frac{\Lambda_{Z'}}{\text{TeV}} \right), |(g_L^d)_{sd}| \lesssim 3.47 \times 10^{-5} \left( \frac{\Lambda_{Z'}}{\text{TeV}} \right). \quad (44)$$

Here, these bounds are given by the requirements that the deviations of  $\Delta M_{B_d}$  and  $|\epsilon_K|$  from the SM predictions are less than 10 %. When  $\epsilon \sim m_s/m_b$ , the small flavor changing couplings are realized as discussed in Eq. (23). The  $\Lambda_{Z'} = \mathcal{O}(10)$  TeV scenario can satisfy these strong upper bounds. Note that the constraint from  $|\epsilon_K|$  can be drastically relaxed if we simply assume that the imaginary part of  $(g_L^d)_{sd}$  is vanishing.

Let us give a comment on the contribution of the scalars to  $B \rightarrow K^* \mu \mu$  in our model. The box diagrams involving the charged Higgs scalar generate the operators, such as

$$\Delta \mathcal{H}_{\text{eff}}^{b-s} = C_{LR}^\mu (\bar{s}_L \gamma_\mu b_L) (\bar{\mu}_R \gamma^\mu \mu_R) + C_{RR}^\mu (\bar{s}_R \gamma_\mu b_R) (\bar{\mu}_R \gamma^\mu \mu_R) + h.c.. \quad (45)$$

In addition, there are box diagrams involving both  $W$  and charged Higgs bosons. Those operators modify our prediction given by  $Z'$  exchange. Those Wilson coefficients are, however, suppressed by the CKM matrix and the fermion masses originated from the Yukawa couplings, even though  $\tan\beta$  enhances each coefficient. The dominant contribution appears in  $C_{LR}^\mu$ , which is proportional to the top quark mass and the large  $G_{tt}$ . The  $B \rightarrow X_s \gamma$  process however constrains  $G_{tt}$  and  $\tan\beta$ . In addition, the Yukawa couplings of charged Higgs with muons are suppressed by the muon mass. Therefore, we would not expect the coefficients to be sizable enough to change our prediction to  $B \rightarrow K^* \mu \mu$ .

### 3.2 $B \rightarrow X_s \gamma$

Based on the above discussion, we study the other flavor violating processes: e.g.,  $B \rightarrow X_s \gamma$  and  $B \rightarrow D^{(*)} \tau \nu$ . Especially, it is known that the former process strictly constrains the extra Higgs contributions.

The branching ratio of  $B \rightarrow X_s \gamma$  has been calculated in 2HDM [85–88]. The relevant operators are

$$\mathcal{H}_{\text{eff}}^{b \rightarrow s \gamma} = -\frac{4G_F}{\sqrt{2}} V_{ts}^* V_{tb} (C_7 \mathcal{O}_7 + C_8 \mathcal{O}_8), \quad (46)$$

where the operators are defined as

$$\mathcal{O}_7 = \frac{e}{16\pi^2} m_b (\bar{s}_L \sigma^{\mu\nu} b_R) F_{\mu\nu}, \quad \mathcal{O}_8 = \frac{g_s}{16\pi^2} m_b (\bar{s}_L t^a \sigma^{\mu\nu} b_R) G_{\mu\nu}^a. \quad (47)$$

In our model, the one-loop corrections involving charged Higgs appear in  $C_7$  and  $C_8$ :

$$C_7 = \left( \frac{m_j^u m_k^u}{m_t^2} \right) \frac{V_{kb} V_{js}^*}{V_{tb} V_{ts}^*} G_{ki}^* G_{ji} C_7^{(1)}(x_i) + \left( \frac{m_k^u}{m_t} \right) \frac{V_{ib} V_{ks}^*}{V_{tb} V_{ts}^*} G_{ki} \tan \beta C_7^{(2)}(x_i), \quad (48)$$

$$C_8 = \left( \frac{m_j^u m_k^u}{m_t^2} \right) \frac{V_{kb} V_{js}^*}{V_{tb} V_{ts}^*} G_{ki}^* G_{ji} C_8^{(1)}(x_i) + \left( \frac{m_k^u}{m_t} \right) \frac{V_{ib} V_{ks}^*}{V_{tb} V_{ts}^*} G_{ki} \tan \beta C_8^{(2)}(x_i). \quad (49)$$

$x_i = (m_i^u/m_{H^\pm})^2$  and the loop functions are given by

$$C_7^{(1)}(x) = \frac{x}{72} \left\{ \frac{-8x^3 + 3x^2 + 12x - 7 + (18x^2 - 12x) \ln x}{(x-1)^4} \right\}, \quad (50)$$

$$C_7^{(2)}(x) = \frac{x}{12} \left\{ \frac{-5x^2 + 8x - 3 + (6x - 4) \ln x}{(x-1)^3} \right\}, \quad (51)$$

$$C_8^{(1)}(x) = \frac{x}{24} \left\{ \frac{-x^3 + 6x^2 - 3x - 2 - 6x \ln x}{(x-1)^4} \right\}, \quad (52)$$

$$C_8^{(2)}(x) = \frac{x}{4} \left\{ \frac{-x^2 + 4x - 3 - 2 \ln x}{(x-1)^3} \right\}. \quad (53)$$

Note that the SM contributions are  $C_7^{\text{SM}} = 3 C_7^{(1)}(m_t^2/M_W^2)$  and  $C_8^{\text{SM}} = 3 C_8^{(1)}(m_t^2/M_W^2)$ .

The branching ratio of  $B \rightarrow X_s \gamma$  has been measured and the result is consistent with the SM prediction. If  $(G_R^u)_{tt}$  is deviated from 1, large  $\tan \beta$  drastically changes the SM prediction because there is a term linear to  $\tan \beta$  in  $(Y_\pm^u)_{ij}$ . In Ref. [6], the allowed region for the new physics contribution to  $C_7$  has been proposed according to the global analysis including  $B \rightarrow K^* l l$ :  $-0.04 \leq C_7 \leq 0$  at the  $1\sigma$  level. In our model,  $C_7$  is almost real and is predicted to be positive, so that too large contributions should be avoided. In Ref. [88], the calculation of the SM prediction for  $B \rightarrow X_s \gamma$  has been done at the NNLO level. Following that result, we obtain our prediction for this process. In order to survey the allowed region in our model, we consider two parameter choices in this section and the next section:

- (A)  $((G_R^u)_{tt}, (G_R^u)_{tc}, (G_R^u)_{cc}, (G_R^u)_{uu}) = (1 - (G_R^u)_{cc}, 0.03, 10^{-3}, 0)$ ,
- (B)  $((G_R^u)_{tt}, (G_R^u)_{tc}, (G_R^u)_{cc}, (G_R^u)_{uu}) = (1 - (G_R^u)_{cc}, -0.3, 0.1, 0)$ .

The parameters in the case (A) correspond to  $\epsilon \simeq 0.03$ , that is predicted by  $m_s/m_b$ , as discussed in Sec. 2. In the case (B),  $(G_R^u)_{tc}$  is fixed to be  $-0.3$  and the behavior of the branching ratio of  $B \rightarrow X_s \gamma$  is totally different from the case (A).

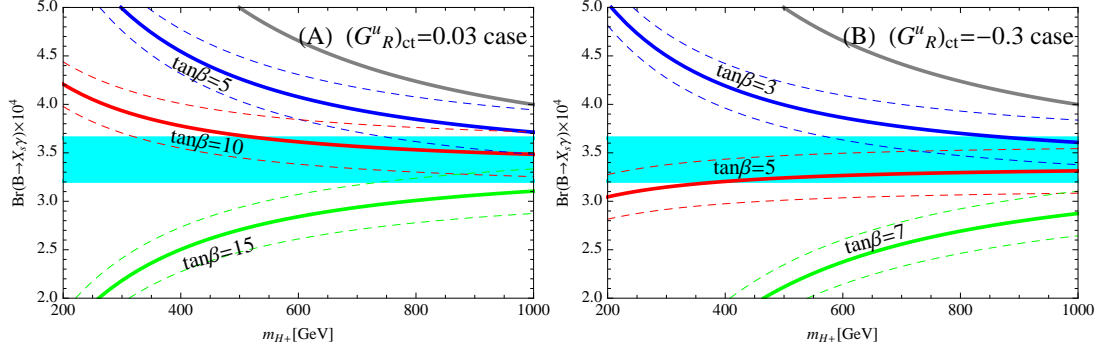


Figure 2: Our predictions of  $\text{Br}(B \rightarrow X_s \gamma)$  in the case (A) and (B).  $\tan \beta$  is fixed at  $\tan \beta = 5$  (Blue), 10 (Red), 15 (Green) in the case (A) and  $\tan \beta = 3$  (Blue), 5 (Red), 7 (Green) in the case (B). The charged Higgs mass within  $200\text{GeV} \leq m_{H_{\pm}} \leq 1.0\text{TeV}$ . The cyan region is the  $1\sigma$  range of the experimental results [83]. The solid gray line corresponds to the  $\tan \beta = 50$  case with  $(G_R^u)_{ct} = -10^{-3}$ .

In Fig. 2, we draw the branching ratios in each case. For this process, an important parameter is  $(Y_{\pm}^u)_{st}$  defined as

$$(Y_{\pm}^u)_{st} \simeq -\frac{m_t \sqrt{2}}{v} V_{ts}^* G_{tt} - \frac{m_c \sqrt{2}}{v} V_{cs}^* G_{ct}. \quad (54)$$

Note that the coupling  $(Y_{\pm}^u)_{st}$  can vanish for different values of  $\tan \beta$  from the cancellation of two terms in Eq. (54), depending on the sign of  $G_{ct}$ .

In the case (A),  $\tan \beta$  is fixed at  $\tan \beta = 5$  (Blue), 10 (Red), and 15 (Green) on each line, respectively. The predictions are drawn in the left panel of Fig. 2. Dashed lines depict the region including  $\pm 1\sigma$  error of the SM prediction for each  $\tan \beta$  case. The cyan band is the  $1\sigma$  region of the combined experimental result [83]. In the case (A), we can see the cancellation between the terms linear to  $G_{tt}$  and  $G_{ct}$  in  $(Y_{\pm}^u)_{st}$ , when  $\tan \beta$  is around 10. Otherwise, the branching ratio deviates significantly from the experimental result unless  $m_{H_{\pm}}$  is heavier than 500 GeV. The solid gray line draws the prediction of the  $G_{ct} = -10^{-3}$  case with  $\tan \beta = 50$ , that is preferred by the excesses in  $R(D^{(*)})$ . The lower bound on the charge Higgs mass reaches 1 TeV, in this large  $\tan \beta$  case. This is very strong, compared to the one in the type-II 2HDM:  $m_{H_{\pm}} > 480$  GeV [88]. This is because there is a  $\tan^2 \beta$  enhancement in Eq. (48). Note that we have ignored the corrections from the light quark masses, so that we need to improve the accuracy related with the light quark masses, if light charged Higgs is observed in the future experiments.

In the case (B),  $\tan \beta$  is chosen as  $\tan \beta = 3$  (Blue), 5 (Red), and 7 (Green) on each line in the right panel of Fig. 2. The behavior is totally different from that in the case (A) because of the negative sign of  $V_{ts}$  in  $(Y_{\pm}^u)_{st}$ . In this case,  $(G_R^u)_{ct}$  is negative, so both terms in Eq. (54) have same sign unless  $\tan \beta$  is small. As shown in Fig. 2,  $\tan \beta \simeq 5$  realizes the cancellation  $(Y_{\pm}^u)_{st}$  and allows the charged Higgs mass to be as light as  $\sim 300$  GeV, which is distinctly different from the usual Type-II 2HDM.

Experiment	$R(D)$	$R(D^*)$
Belle	$0.375 \pm 0.064 \pm 0.026$ [14]	$0.302 \pm 0.03 \pm 0.011$ [15]
BaBar	$0.440 \pm 0.058 \pm 0.042$ [12, 13]	$0.332 \pm 0.024 \pm 0.018$ [12, 13]
LHCb		$0.336 \pm 0.027 \pm 0.030$ [94]
HFAG	$0.397 \pm 0.040 \pm 0.028$ [83]	$0.316 \pm 0.016 \pm 0.010$ [83]
SM prediction	$0.300 \pm 0.008$ [89–92]	$0.252 \pm 0.003$ [93]

Table 3: Summary of the experimental results in  $B \rightarrow D^{(*)}\tau\nu$  decays.

In the next section, we discuss  $B \rightarrow D^{(*)}\tau\nu$ , where the deviations from the SM predictions have been reported in the experiments, as shown in Table 3. The excess may require light charged Higgs boson. Therefore, we study the semileptonic  $B$  decay,  $B \rightarrow D^{(*)}\tau\nu$ , in each case, and discuss our predictions to the observables in the processes.

### 3.3 $R(D)$ and $R(D^*)$

Next, we investigate the semileptonic decays,  $B \rightarrow D^{(*)}\tau\nu$ , where the deviations from the SM predictions have been reported in the observables concerned with the lepton flavor universality. The interesting measurements are the ratios of the branching ratios for  $B \rightarrow D^{(*)}\tau\nu$  to  $B \rightarrow D^{(*)}l\nu$  ( $l = e, \mu$ ),

$$R(D^{(*)}) = \frac{\text{Br}(B \rightarrow D^{(*)}\tau\nu)}{\text{Br}(B \rightarrow D^{(*)}l\nu)}. \quad (55)$$

In the SM,  $R(D) = 0.300 \pm 0.008$  [89–92] and  $R(D^*) = 0.252 \pm 0.003$  [93]. The experimental results and the SM predictions are summarized in Table 3, and we find the discrepancies over  $2\sigma$ .

The semileptonic decays are given by the following operators:

$$\mathcal{H}_{\text{eff}}^{B \rightarrow \tau} = C_{\text{SM}}^{cb}(\bar{c}_L \gamma_\mu b_L)(\bar{\tau}_L \gamma^\mu \nu_L) + C_R^{cb}(\bar{c}_L b_R)(\bar{\tau}_R \nu_L) + C_L^{cb}(\bar{c}_R b_L)(\bar{\tau}_R \nu_L), \quad (56)$$

where  $C_{\text{SM}}^{cb}$  is the Wilson coefficient in the SM and  $C_{R,L}^{cb}$  are generated by the charged Higgs exchange in our model. In Ref. [59], the simplified expressions for  $R(D^{(*)})$  have been proposed:

$$R(D) = R_{\text{SM}} \left( 1 + 1.5 \text{Re} \left( \frac{C_R^{cb} + C_L^{cb}}{C_{\text{SM}}^{cb}} \right) + \left| \frac{C_R^{cb} + C_L^{cb}}{C_{\text{SM}}^{cb}} \right|^2 \right), \quad (57)$$

$$R(D^*) = R_{\text{SM}}^* \left( 1 + 0.12 \text{Re} \left( \frac{C_R^{cb} - C_L^{cb}}{C_{\text{SM}}^{cb}} \right) + 0.05 \left| \frac{C_R^{cb} - C_L^{cb}}{C_{\text{SM}}^{cb}} \right|^2 \right), \quad (58)$$

where each Wilson coefficient is at the  $B$  meson scale [16]. Here,  $R_{\text{SM}}^{(*)}$  are the SM predictions.

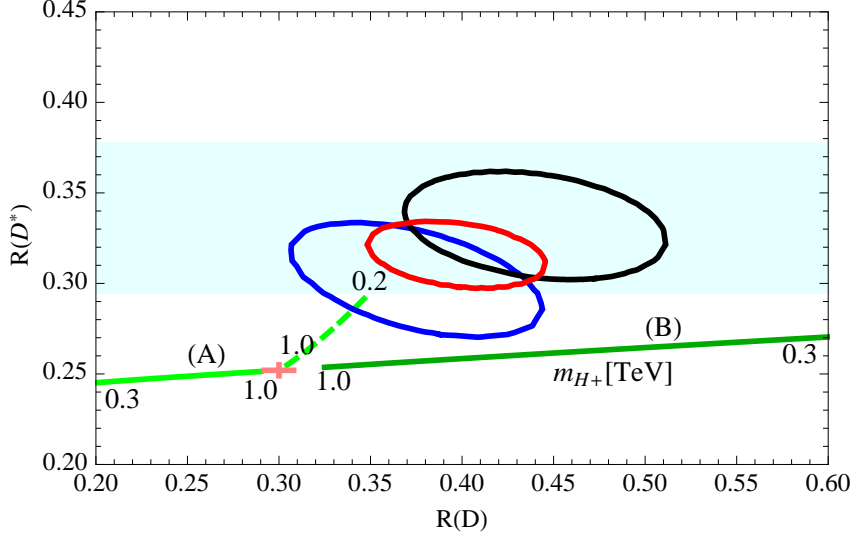


Figure 3:  $R(D)$  vs.  $R(D^*)$  in the cases (A) (light green) and (B) (dark green).  $\tan \beta$  is fixed at  $\tan \beta = 10$  in the case (A) and  $\tan \beta = 5$  in the case (B). The charged Higgs mass is within  $300 \text{ GeV} \leq m_{H_{\pm}} \leq 1.0 \text{ TeV}$  on each line. The dashed line corresponds to the case with  $(G_R^u)_{ct} = 10^{-3}$ ,  $\tan \beta = 50$  and  $200 \text{ GeV} \leq m_{H_{\pm}} \leq 1.0 \text{ TeV}$ . Each ellipse describes the  $1\sigma$  results at the Belle (blue) [14, 15], BaBar (black) [12, 13], LHCb (cyan band) [94] experiments and HFAG (red) [83], respectively. The pink lines correspond the SM predictions within  $1\sigma$  [92, 93].

Integrating out the charged Higgs in our model, we obtain the Wilson coefficients as

$$C_{\text{SM}}^{cb} = 2V_{cb}/v^2, \quad (59)$$

$$\frac{C_L^{cb}}{C_{\text{SM}}^{cb}} = \frac{m_c m_\tau}{m_{H_{\pm}}^2} \tan^2 \beta - \sum_k \frac{V_{kb}}{V_{cb}} \frac{m_k^u m_\tau (G_R^u)_{kc}^*}{m_{H_{\pm}}^2 \cos^2 \beta}, \quad (60)$$

$$\frac{C_R^{cb}}{C_{\text{SM}}^{cb}} = -\frac{m_b m_\tau}{m_{H_{\pm}}^2} \tan^2 \beta. \quad (61)$$

Fig. 3 shows our predictions of  $R(D^{(*)})$  in the cases (A) and (B). We fix  $\tan \beta = 10$  in the case (A) and  $\tan \beta = 5$  in the case (B), respectively, in order to satisfy  $B \rightarrow X_s \gamma$  constraint even in the light charge Higgs mass region. Each ellipse describes the  $1\sigma$  results at the Belle (blue) [14, 15], BaBar (black) [12, 13], LHCb (cyan band) [94] experiments and HFAG (red) [83], respectively. The pink lines correspond the SM predictions within  $1\sigma$  [92, 93].

The light green line corresponds to the prediction of the case (A). The charged Higgs mass varies between  $300 \text{ GeV} \leq m_{H_{\pm}} \leq 1.0 \text{ TeV}$  from the left to the right on the line. When  $(G_R^u)_{tc}$  is negative,  $C_L^{cb}$  also becomes negative, unless the magnitude of  $(G_R^u)_{tc}$  is quite small. Then, we find that both  $R(D)$  and  $R(D^*)$  tend to be smaller than the SM predictions.



The dark green line depicts the prediction of the case (B). The charged Higgs mass varies from right to left on the line between  $300 \text{ GeV} \leq m_{H_{\pm}} \leq 1.0 \text{ TeV}$ . In contrast to the case (A), we see that  $R(D)$  in particular can be enhanced a lot compared with the SM prediction. On the other hand, the enhancement of  $R(D^*)$  is rather small, compared to the experimental results.

The dashed line describes the prediction, when  $(G_R^u)_{ct} = -10^{-3}$  and  $\tan \beta = 50$  are satisfied. The charged Higgs mass is in the range of  $200 \text{ GeV} \leq m_{H_{\pm}} \leq 1.0 \text{ TeV}$ . In this case, large  $\tan \beta$  induces an enhancement in  $C_R^{cb}$ , as well as in  $C_L^{cb}$ . Both coefficients are comparable, and this parameter choice can enhance both  $R(D)$  and  $R(D^*)$ . The experimental results, however, require  $\mathcal{O}(100) \text{ GeV}$  charged Higgs mass, and the constraint from  $B \rightarrow X_s \gamma$  does not allow such a light charged Higgs scenario. (See the solid gray line in Fig. 2 for the predictions of  $B(B \rightarrow X_s \gamma)$ .)

Recently, there is a proposal that the lifetime of  $B_c$  can severely constrain the explanation of  $B \rightarrow D^* \tau \nu$  [95], which heavily relies on the lattice calculation of the  $B_c$  meson decay constant. It is shown that accommodation with  $R(D^*)$  using charged Higgs fields may be in tension with the observables in the leptonic decay  $B_c \rightarrow \tau \nu$  [95]. However, our model would evade the strong bound from  $B_c \rightarrow \tau \nu$  because it predicts small enhancement in the  $B \rightarrow D^* \tau \nu$ . On the other hand, our model would be excluded, if these excesses in the semileptonic decays  $B \rightarrow D^{(*)} \tau \nu$  are confirmed to be the signals of new physics in the future.

### 3.4 Exotic top decay

In our model, there are FCNCs involving top and charm quarks, as shown in Eq. (35). The mixing parameter  $(G_R^u)_{tc}$  is estimated to be about  $\mathcal{O}(0.01)$ . However, the FCNCs of the neutral scalars may have enhancements from large  $\tan \beta$  and top quark mass, so that the flavor violating top decay,  $t \rightarrow ch$  might significantly become large. The couplings relevant to the top decay are approximately evaluated as

$$\frac{m_t}{v} \tan \beta (G_R^u)_{tc} \{ \sin(\alpha - \beta) h + \cos(\alpha - \beta) H - iA \} \bar{t}_L c_R + h.c.. \quad (62)$$

The EWPOs require the SM limit that  $\cos(\alpha - \beta)$  is close to unity, so that the flavor violating coupling of  $h$ , whose mass is 125 GeV, vanishes in this limit.

The exotic top decay,  $t \rightarrow h c$ , has been investigated at the LHC experiments [96, 97]. The upper bound on the Yukawa couplings between top and charm quarks is about 0.1. Then, our model is still safe for the constraint, as far as  $\sin(\alpha - \beta)$  is less than  $\mathcal{O}(0.1)$ .

Note that  $(G_R^u)_{tu}$  is smaller than  $(G_R^u)_{tc}$  following Eq. (35), so that the same-sign top signal,  $pp \rightarrow tt$ , is highly suppressed in the current model, unlike the models considered in Refs. [9–11].

Fields	spin	SU(3) <sub>c</sub>	SU(2) <sub>L</sub>	U(1) <sub>Y</sub>	U(1)'
$Q'_R$	1/2	<b>3</b>	<b>2</b>	1/6	1
$Q'_L$	1/2	<b>3</b>	<b>2</b>	1/6	0
$u'_L$	1/2	<b>3</b>	<b>1</b>	2/3	1
$u'_R$	1/2	<b>3</b>	<b>1</b>	2/3	0
$u''_L$	1/2	<b>3</b>	<b>1</b>	2/3	1 + q <sub>3</sub>
$u''_R$	1/2	<b>3</b>	<b>1</b>	2/3	0
$R'_\mu$	1/2	<b>1</b>	<b>2</b>	-1/2	q <sub>e</sub>
$L'_\mu$	1/2	<b>1</b>	<b>2</b>	-1/2	0
$R'_\tau$	1/2	<b>1</b>	<b>2</b>	-1/2	q <sub>e</sub>
$L'_\tau$	1/2	<b>1</b>	<b>2</b>	-1/2	0
$\mu'_L$	1/2	<b>1</b>	<b>1</b>	-1	q <sub>e</sub> - 1
$\mu'_R$	1/2	<b>1</b>	<b>1</b>	-1	0
$\tau'_L$	1/2	<b>1</b>	<b>1</b>	-1	q <sub>e</sub> - 1
$\tau'_R$	1/2	<b>1</b>	<b>1</b>	-1	0
$\Phi_l$	0	<b>1</b>	<b>1</b>	0	q <sub>e</sub>
$\Phi_r$	0	<b>1</b>	<b>1</b>	0	q <sub>e</sub> - 1

Table 4: The extra chiral fermions for the anomaly-free conditions with  $(q_1, q_2) = (0, 1)$ .

## 4 Extra matter fields

In our model, we considered extra U(1)' flavor symmetry under which the SM fermions are chirally charged, and so we have to introduce extra chiral fermions in order to achieve the anomaly-free conditions. There are several possibilities for the field contents. For instance, the additional fermions with the charge assignment in Table 4 lead to the anomaly-free U(1)' gauge symmetry.

Now, we write down the Yukawa couplings for the extra fermions involving  $\Phi$  and  $H_i$ :

$$V_{\text{extra}} = y'_Q \overline{Q'_R} \Phi Q'_L + y'_u \overline{u'_L} \Phi u'_R + y' \overline{Q'_R} \tilde{H}_3 u''_L + y'' \overline{Q'_L} \tilde{H}_1 u''_R + \dots + h.c. \quad (63)$$

In order to write down the mass terms for the extra fermions, we may have to introduce extra complex scalars which are SM singlets and carry U(1)' charges. For instance, we can write down the mass terms for the extra leptons and quarks as

$$y'_\mu \overline{R'_\mu} \Phi_l L'_\mu + y'_\tau \overline{R'_\tau} \Phi_l L'_\tau + y''_\mu \overline{\mu'_L} \Phi_r \mu'_R + y''_\tau \overline{\tau'_L} \Phi_r \tau'_R + y''_u \overline{u''_L} \Phi_r^\dagger u''_R, \quad (64)$$

where  $q_e = -q_3$  is assumed.

In this setup,  $Q'_L$  is not distinguished with  $Q_L^i$ , so that we can write down the Yukawa terms,  $\overline{Q'_L} \widetilde{H}_1 \hat{u}_R^a$ , which causes the mass mixing between the extra quarks and the SM quarks. We assume that the extra fermions are heavy, so that the mixing effect is not relevant to our analysis. In any case, the extra quarks can decay through the mixing.

Similarly, we can also find the mixing terms in the lepton sector. For instance,  $L'_{\mu,\tau}$  carry the same charges as  $\hat{L}^1$ , so that the Yukawa couplings,  $\overline{L'_{\mu,\tau}} H_1 e_R$  are allowed. If we forbid the mass mixing terms, we will obtain dark matter candidates: that is, the neutral components of  $R'_{\mu,\tau}$  and  $L'_{\mu,\tau}$ .

Another important issue is how to obtain tiny neutrino masses and large lepton mixing. The flavor symmetry limits the Majorana mass matrix for right-handed neutrino,  $\nu_R^i$ , if non-trivial  $U(1)'$  charges are assigned to  $\nu_R^i$ . When  $\nu_R^i$  is neutral under  $U(1)'$  and  $q_e$  is defined as  $q_e = -q_3$ , we can write down the Yukawa couplings for the neutrino masses as

$$y_{1i}^\nu \overline{L^1} \widetilde{H}_1 \nu_R^i + y_{2i}^\nu \overline{L^2} \widetilde{H}_3 \nu_R^i + y_{3i}^\nu \overline{L^3} \widetilde{H}_3 \nu_R^i + h.c.. \quad (65)$$

Note that the Majorana masses of  $\nu_R^i$  are also allowed by the flavor symmetry. Detailed study of phenomenology involving the exotic fermions are beyond the scope of this paper, and are left for future study.

## 5 Summary

In this paper, we propose an extension of the SM with  $U(1)'$  flavor gauge symmetry, motivated by the fermion mass hierarchy and the LHCb anomaly. In our model,  $U(1)'$  charges are assigned to the SM fermions, and flavored Higgs doublets are introduced to obtain the observed fermion mass hierarchy. The alignment of the Yukawa couplings is controlled by the  $U(1)'$  flavor symmetry, and the VEV alignment of the Higgs doublets realizes the realistic mass matrices for the observed fermions.

Moreover, the charge assignment in Table 1 can evade the strong bounds from the Drell-Yan process and the lepton flavor violating  $\mu$  and  $\tau$  decays. We can also explain the LHCb anomaly in the  $B \rightarrow K^* \ell \ell$ , without conflict with the  $B_s - \overline{B}_s$  mixing which is the strongest bound in our model.

In this setup, relatively large  $(t, c)$ -elements of the Yukawa couplings of the neutral scalar Higgs bosons are predicted. This coupling relates to the  $(b, c)$ -element of the charged Higgs Yukawa coupling, so that we have also investigated  $R(D^{(*)})$ , where the significant deviations from the SM predictions are reported by the Belle and BaBar collaborations.  $R(D)$  is easily enhanced by the  $(b, c)$  coupling, but  $R(D^*)$  cannot be large because of the stringent bound from  $B \rightarrow X_s \gamma$ . In fact, the strong constraint from the  $B \rightarrow X_s \gamma$  is very strict, if the charged Higgs mass is less than 1 TeV. If we require vanishing  $(Y_\pm^u)_{st}$ , we could discuss light charged Higgs mass, but we need more precise calculation, including light quark mass contribution. We also discussed the flavor violating decay of top quark. If the sensitivity of the LHC experiment to the  $(t, c)$ -Yukawa coupling reaches  $\mathcal{O}(0.01)$ , we could test our model in this process.

Recently, the search for heavy scalar particles is well developed in the LHC experiments. Our predictions against the heavy resonance search are similar to the ones of the type-II 2HDM, so that the direct search for the scalar fields will be a good process to test our model, although  $\tan \beta \sim \mathcal{O}(10)$  is currently allowed as far as  $m_A$  is heavier than 300 GeV [98].

## Acknowledgments

We are grateful to Seungwon Baek, Takaaki Nomura, and Yeo Woong Yoon for useful comments on the subject presented in this paper. This work is supported in part by National Research Foundation of Korea (NRF) Research Grant NRF-2015R1A2A1A05001869 (PK), by the NRF grant funded by the Korea government (MSIP) (No. 2009-0083526) through Korea Neutrino Research Center at Seoul National University (PK), and by the Do-Yak project of NRF under Contract No. NRF-2015R1A2A1A15054533 (CY). The work of Y.S. is supported by the Japan Society for the Promotion of Science (JSPS) Research Fellowships for Young Scientists, No. 16J08299.

## References

- [1] C. D. Froggatt and H. B. Nielsen, Nucl. Phys. B **147** (1979) 277.
- [2] R. Aaij *et al.* [LHCb Collaboration], Phys. Rev. Lett. **113**, 151601 (2014) [arXiv:1406.6482 [hep-ex]].
- [3] R. Aaij *et al.* [LHCb Collaboration], Phys. Rev. Lett. **111**, 191801 (2013) [arXiv:1308.1707 [hep-ex]].
- [4] R. Aaij *et al.* [LHCb Collaboration], JHEP **1602**, 104 (2016) [arXiv:1512.04442 [hep-ex]].
- [5] G. Hiller and M. Schmaltz, Phys. Rev. D **90**, 054014 (2014) [arXiv:1408.1627 [hep-ph]].
- [6] S. Descotes-Genon, L. Hofer, J. Matias and J. Virto, JHEP **1606**, 092 (2016) [arXiv:1510.04239 [hep-ph]].
- [7] W. Altmannshofer and D. M. Straub, arXiv:1503.06199 [hep-ph].
- [8] T. Hurth, F. Mahmoudi and S. Neshatpour, Nucl. Phys. B **909**, 737 (2016) [arXiv:1603.00865 [hep-ph]].
- [9] P. Ko, Y. Omura and C. Yu, Phys. Rev. D **85**, 115010 (2012) [arXiv:1108.0350 [hep-ph]].
- [10] P. Ko, Y. Omura and C. Yu, JHEP **1201**, 147 (2012) [arXiv:1108.4005 [hep-ph]].

- [11] P. Ko, Y. Omura and C. Yu, Eur. Phys. J. C **73**, no. 1, 2269 (2013) [arXiv:1205.0407 [hep-ph]].
- [12] J. P. Lees *et al.* [BaBar Collaboration], Phys. Rev. Lett. **109**, 101802 (2012) [arXiv:1205.5442 [hep-ex]].
- [13] J. P. Lees *et al.* [BaBar Collaboration], Phys. Rev. D **88**, no. 7, 072012 (2013) [arXiv:1303.0571 [hep-ex]].
- [14] M. Huschle *et al.* [Belle Collaboration], Phys. Rev. D **92**, no. 7, 072014 (2015) [arXiv:1507.03233 [hep-ex]].
- [15] A. Abdesselam *et al.* [Belle Collaboration], arXiv:1603.06711 [hep-ex].
- [16] A. Datta, M. Duraisamy and D. Ghosh, Phys. Rev. D **86**, 034027 (2012) [arXiv:1206.3760 [hep-ph]].
- [17] X. G. He and G. Valencia, Phys. Rev. D **87**, no. 1, 014014 (2013) [arXiv:1211.0348 [hep-ph]].
- [18] P. Biancofiore, P. Colangelo and F. De Fazio, Phys. Rev. D **87**, no. 7, 074010 (2013) [arXiv:1302.1042 [hep-ph]].
- [19] I. Doršner, S. Fajfer, N. Košnik and I. Nišandžić, JHEP **1311**, 084 (2013) [arXiv:1306.6493 [hep-ph]].
- [20] Y. Sakaki, M. Tanaka, A. Tayduganov and R. Watanabe, Phys. Rev. D **88**, no. 9, 094012 (2013) [arXiv:1309.0301 [hep-ph]].
- [21] A. Abada, A. M. Teixeira, A. Vicente and C. Weiland, JHEP **1402**, 091 (2014) [arXiv:1311.2830 [hep-ph]].
- [22] K. Hagiwara, M. M. Nojiri and Y. Sakaki, Phys. Rev. D **89**, no. 9, 094009 (2014) [arXiv:1403.5892 [hep-ph]].
- [23] M. Duraisamy, P. Sharma and A. Datta, Phys. Rev. D **90**, no. 7, 074013 (2014) [arXiv:1405.3719 [hep-ph]].
- [24] Y. Sakaki, M. Tanaka, A. Tayduganov and R. Watanabe, Phys. Rev. D **91**, no. 11, 114028 (2015) [arXiv:1412.3761 [hep-ph]].
- [25] B. Bhattacharya, A. Datta, D. London and S. Shivashankara, Phys. Lett. B **742**, 370 (2015) [arXiv:1412.7164 [hep-ph]].
- [26] R. Alonso, B. Grinstein and J. Martin Camalich, JHEP **1510**, 184 (2015) [arXiv:1505.05164 [hep-ph]].
- [27] A. Greljo, G. Isidori and D. Marzocca, JHEP **1507**, 142 (2015) [arXiv:1506.01705 [hep-ph]].

- [28] L. Calibbi, A. Crivellin and T. Ota, Phys. Rev. Lett. **115**, 181801 (2015) doi:10.1103/PhysRevLett.115.181801 [arXiv:1506.02661 [hep-ph]].
- [29] M. Freytsis, Z. Ligeti and J. T. Ruderman, Phys. Rev. D **92**, no. 5, 054018 (2015) [arXiv:1506.08896 [hep-ph]].
- [30] M. Bauer and M. Neubert, Phys. Rev. Lett. **116**, no. 14, 141802 (2016) [arXiv:1511.01900 [hep-ph]].
- [31] C. Hati, G. Kumar and N. Mahajan, JHEP **1601**, 117 (2016) [arXiv:1511.03290 [hep-ph]].
- [32] R. Barbieri, G. Isidori, A. Pattori and F. Senia, Eur. Phys. J. C **76**, no. 2, 67 (2016) [arXiv:1512.01560 [hep-ph]].
- [33] D. Becirevic, S. Fajfer, I. Nisandzic and A. Tayduganov, arXiv:1602.03030 [hep-ph].
- [34] R. Alonso, A. Kobach and J. Martin Camalich, Phys. Rev. D **94**, no. 9, 094021 (2016) [arXiv:1602.07671 [hep-ph]].
- [35] B. Dumont, K. Nishiwaki and R. Watanabe, Phys. Rev. D **94**, no. 3, 034001 (2016) [arXiv:1603.05248 [hep-ph]].
- [36] S. M. Boucenna, A. Celis, J. Fuentes-Martin, A. Vicente and J. Virto, Phys. Lett. B **760**, 214 (2016) [arXiv:1604.03088 [hep-ph]].
- [37] D. Boubaa, S. Khalil and S. Moretti, arXiv:1604.03416 [hep-ph].
- [38] D. Das, C. Hati, G. Kumar and N. Mahajan, Phys. Rev. D **94**, 055034 (2016) [arXiv:1605.06313 [hep-ph]].
- [39] X. Q. Li, Y. D. Yang and X. Zhang, JHEP **1608**, 054 (2016) [arXiv:1605.09308 [hep-ph]].
- [40] F. Feruglio, P. Paradisi and A. Pattori, Phys. Rev. Lett. **118**, no. 1, 011801 (2017) [arXiv:1606.00524 [hep-ph]].
- [41] A. K. Alok, D. Kumar, S. Kumbhakar and S. U. Sankar, arXiv:1606.03164 [hep-ph].
- [42] S. M. Boucenna, A. Celis, J. Fuentes-Martin, A. Vicente and J. Virto, JHEP **1612**, 059 (2016) [arXiv:1608.01349 [hep-ph]].
- [43] N. G. Deshpande and X. G. He, arXiv:1608.04817 [hep-ph].
- [44] D. Bećirević, S. Fajfer, N. Košnik and O. Sumensari, Phys. Rev. D **94**, no. 11, 115021 (2016) [arXiv:1608.08501 [hep-ph]].
- [45] S. Sahoo, R. Mohanta and A. K. Giri, Phys. Rev. D **95**, 035027 (2017) [arXiv:1609.04367 [hep-ph]].

- [46] G. Hiller, D. Loose and K. Schonwald, JHEP **1612**, 027 (2016) [arXiv:1609.08895 [hep-ph]].
- [47] B. Bhattacharya, A. Datta, J. P. Guevin, D. London and R. Watanabe, JHEP **1701**, 015 (2017) [arXiv:1609.09078 [hep-ph]].
- [48] Z. Ligeti, M. Papucci and D. J. Robinson, JHEP **1701**, 083 (2017) [arXiv:1610.02045 [hep-ph]].
- [49] D. Bardhan, P. Byakti and D. Ghosh, JHEP **1701**, 125 (2017) [arXiv:1610.03038 [hep-ph]].
- [50] R. Dutta and A. Bhol, arXiv:1611.00231 [hep-ph].
- [51] S. Bhattacharya, S. Nandi and S. K. Patra, arXiv:1611.04605 [hep-ph].
- [52] R. Barbieri, C. W. Murphy and F. Senia, Eur. Phys. J. C **77**, no. 1, 8 (2017) [arXiv:1611.04930 [hep-ph]].
- [53] L. T. Hue, A. B. Arbuzov, N. T. K. Ngan and H. N. Long, arXiv:1611.06801 [hep-ph].
- [54] M. A. Ivanov, J. G. Korner and C. T. Tran, arXiv:1701.02937 [hep-ph].
- [55] R. Dutta and A. Bhol, arXiv:1701.08598 [hep-ph].
- [56] R. Alonso, J. Martin Camalich and S. Westhoff, arXiv:1702.02773 [hep-ph].
- [57] G. Cvetič, F. Halzen, C. S. Kim and S. Oh, arXiv:1702.04335 [hep-ph].
- [58] C. T. Tran, M. A. Ivanov and J. G. Korner, arXiv:1702.06910 [hep-ph].
- [59] A. Crivellin, C. Greub and A. Kokulu, Phys. Rev. D **86**, 054014 (2012) [arXiv:1206.2634 [hep-ph]].
- [60] P. Ko, Y. Omura and C. Yu, JHEP **1303**, 151 (2013) [arXiv:1212.4607 [hep-ph]].
- [61] C. S. Kim, Y. W. Yoon and X. B. Yuan, JHEP **1512**, 038 (2015) [arXiv:1509.00491 [hep-ph]].
- [62] S. Fajfer, J. F. Kamenik, I. Nisandzic and J. Zupan, Phys. Rev. Lett. **109**, 161801 (2012) [arXiv:1206.1872 [hep-ph]].
- [63] A. Celis, M. Jung, X. Q. Li and A. Pich, JHEP **1301**, 054 (2013) [arXiv:1210.8443 [hep-ph]].
- [64] M. Tanaka and R. Watanabe, Phys. Rev. D **87**, no. 3, 034028 (2013) [arXiv:1212.1878 [hep-ph]].
- [65] A. Crivellin, A. Kokulu and C. Greub, Phys. Rev. D **87**, no. 9, 094031 (2013) [arXiv:1303.5877 [hep-ph]].

- [66] A. Crivellin, J. Heeck and P. Stoffer, Phys. Rev. Lett. **116**, no. 8, 081801 (2016) [arXiv:1507.07567 [hep-ph]].
- [67] T. Enomoto and R. Watanabe, JHEP **1605**, 002 (2016) [arXiv:1511.05066 [hep-ph]].
- [68] J. M. Cline, Phys. Rev. D **93**, no. 7, 075017 (2016) [arXiv:1512.02210 [hep-ph]].
- [69] L. Wang, J. M. Yang and Y. Zhang, arXiv:1610.05681 [hep-ph].
- [70] A. Celis, M. Jung, X. Q. Li and A. Pich, arXiv:1612.07757 [hep-ph].
- [71] C. Patrignani *et al.* [Particle Data Group], Chin. Phys. C **40**, no. 10, 100001 (2016).
- [72] P. Ko, Y. Omura and C. Yu, JHEP **1401**, 016 (2014) [arXiv:1309.7156 [hep-ph]].
- [73] A. Crivellin, G. D'Ambrosio and J. Heeck, Phys. Rev. D **91**, no. 7, 075006 (2015) [arXiv:1503.03477 [hep-ph]].
- [74] W. Altmannshofer and I. Yavin, Phys. Rev. D **92**, no. 7, 075022 (2015) [arXiv:1508.07009 [hep-ph]].
- [75] I. Garcia Garcia, arXiv:1611.03507 [hep-ph].
- [76] P. Ko, T. Nomura and H. Okada, arXiv:1701.05788 [hep-ph].
- [77] P. Ko, T. Nomura and H. Okada, arXiv:1702.02699 [hep-ph].
- [78] S. Baek, J. H. Jeon and C. S. Kim, Phys. Lett. B **664**, 84 (2008) [arXiv:0803.0062 [hep-ph]].
- [79] X. Q. Li, Y. M. Li, G. R. Lu and F. Su, JHEP **1205**, 049 (2012) [arXiv:1204.5250 [hep-ph]].
- [80] Y. Li, W. L. Wang, D. S. Du, Z. H. Li and H. X. Xu, Eur. Phys. J. C **75**, no. 7, 328 (2015) [arXiv:1503.00114 [hep-ph]].
- [81] A. J. Buras, hep-ph/9806471.
- [82] S. Aoki *et al.*, Eur. Phys. J. C **77**, no. 2, 112 (2017) [arXiv:1607.00299 [hep-lat]].
- [83] Y. Amhis *et al.* [Heavy Flavor Averaging Group (HFAG)], arXiv:1412.7515 [hep-ex].
- [84] A. J. Buras, P. H. Chankowski, J. Rosiek and L. Slawianowska, Nucl. Phys. B **619**, 434 (2001) [hep-ph/0107048].
- [85] F. Borzumati and C. Greub, Phys. Rev. D **58**, 074004 (1998) [hep-ph/9802391].
- [86] F. Borzumati and C. Greub, Phys. Rev. D **59**, 057501 (1999) [hep-ph/9809438].



- [87] T. Hermann, M. Misiak and M. Steinhauser, JHEP **1211**, 036 (2012) [arXiv:1208.2788 [hep-ph]].
- [88] M. Misiak *et al.*, Phys. Rev. Lett. **114**, no. 22, 221801 (2015) [arXiv:1503.01789 [hep-ph]].
- [89] J. F. Kamenik and F. Mescia, Phys. Rev. D **78**, 014003 (2008) [arXiv:0802.3790 [hep-ph]].
- [90] M. Tanaka and R. Watanabe, Phys. Rev. D **82**, 034027 (2010) [arXiv:1005.4306 [hep-ph]].
- [91] J. A. Bailey *et al.* [MILC Collaboration], Phys. Rev. D **92**, no. 3, 034506 (2015) [arXiv:1503.07237 [hep-lat]].
- [92] H. Na *et al.* [HPQCD Collaboration], Phys. Rev. D **92**, no. 5, 054510 (2015) Erratum: [Phys. Rev. D **93**, no. 11, 119906 (2016)] [arXiv:1505.03925 [hep-lat]].
- [93] S. Fajfer, J. F. Kamenik and I. Nisandzic, Phys. Rev. D **85**, 094025 (2012) [arXiv:1203.2654 [hep-ph]].
- [94] R. Aaij *et al.* [LHCb Collaboration], Phys. Rev. Lett. **115**, no. 11, 111803 (2015) Addendum: [Phys. Rev. Lett. **115**, no. 15, 159901 (2015)] [arXiv:1506.08614 [hep-ex]].
- [95] R. Alonso, B. Grinstein and J. Martin Camalich, arXiv:1611.06676 [hep-ph].
- [96] G. Aad *et al.* [ATLAS Collaboration], JHEP **1512**, 061 (2015) [arXiv:1509.06047 [hep-ex]].
- [97] V. Khachatryan *et al.* [CMS Collaboration], JHEP **1702**, 079 (2017) [arXiv:1610.04857 [hep-ex]].
- [98] M. Aaboud *et al.* [ATLAS Collaboration], Eur. Phys. J. C **76**, no. 11, 585 (2016) [arXiv:1608.00890 [hep-ex]].